

The Use of Strainmeters to Study Oscillation Processes in a Wide Frequency Range

V. Yu. Timofeev^{a,*}, D. G. Ardyukov^a, A. V. Timofeev^a, E. V. Boyko^a, V. M. Semibalamut^b,
Y. N. Fomin^b, S. V. Panov^c, and M. D. Parushkin^c

^a*Trofimuk Institute of Petroleum Geology and Geophysics, Siberian Branch, Russian Academy of Sciences,
Novosibirsk, 630090 Russia*

^b*Federal Research Center Geophysical Survey, Siberian Branch, Russian Academy of Sciences, Novosibirsk, 630090 Russia*

^c*Institute of Laser Physics, Siberian Branch, Russian Academy of Sciences, Novosibirsk, 630090 Russia*

*e-mail: timofeevy@ipgg.sbras.ru

Abstract—Adit-based linear strain measurements made with strainmeters 1 to 100 m long allow oscillation processes to be studied in a wide range: from a few tens of hertz to several years. Both seismic waves from earthquakes and long-period oscillatory signals are recorded, related to tectonic processes. The paper describes measurements made with rod and laser strain metering systems in an adit of the Talaya seismic station (coordinates 51.68° N, 103.65° E, Lake Baikal Region). The elastic moduli of rocks were evaluated using strainmeter, microbarograph data, and petrophysical core analysis. The Earth's integral rheological parameters, through the Earth's free and tidal oscillations, are calculated. Our findings are in good agreement with modern models of the Earth's internal structure. The paper describes coseismic and long-term volumetric strain variations induced by large regional earthquakes.

Keywords: rod strainmeter, laser strainmeter, Baikal region, seiches in Lake Baikal, Earth's free and tidal oscillations, earthquakes, volumetric strain variations

DOI: 10.3103/S0747923920040106

INTRODUCTION

Strainmeters have been used in studying crustal deformations since the 1900s. Rod (quartz/invar) strainmeters with a baseline of up to 50 m, allow the detection of deformations on the order of 10^{-7} – 10^{-10} (Benioff, 1935; Latynina and Karmaleeva, 1978; Melchior, 1966). Open- and closed-type strainmeters have been created, with the advent of lasers; in the latter case, the laser beam travels toward a reflector in a vacuum pipe. Closed-type systems up to 800 m long, can detect signals from earthquakes and nuclear explosions as well as tidal variations provided that the land topography is flat (Beaumont and Berger, 1974).

Strain measurement techniques are used to solve different problems of geology and geophysics at various spatial and temporal scales: the investigation of seismic wave propagation (Chupin, 2019), the noise of various origins, free oscillations of the Earth (Jahr et al., 2006), the structure of our planet, the free oscillations of the solid and liquid cores of the Earth, and tidal effects; the research into modern tectonic deformations and seismicity; and the assessment of anthropogenic impacts on the geological environment. In seismically active regions, strainmeters are widely used, with a prospect of earthquake prediction (Guseva, 1986; Agnew, 1986; Timofeev et al., 2020).

Under certain conditions, deformation on the order of 10^{-9} – 10^{-11} , can be detected. The places where strainmeters are installed must satisfy the following requirements. First, the influence of surface temperature should be eliminated; that is why strain measurements should be carried out at a depth of 50 m or more. The effects of temperature are minimal when the land topography is flat (Boyarsky et al., 2003) and the most significant in the rugged mountainous areas. Anomalies arise due to the ruggedness and color of the Earth's surface and differences in the thermal diffusivity of rocks (Popov, 1961). Second, having a stable temperature in an adit is the key to ensuring high-precision measurements. We carried out our measurements in a 90-m long adit of the Talaya seismic station located in a mountainous area, at a distance of 7 km from the southwestern end of Lake Baikal (Fig. 1 a).

The average annual temperature is $+1 \pm 1^\circ\text{C}$ in the Talaya adit (Fig. 2); the daily variation at strainmeter sites is 0.001° . Temperature perturbation due to adit attendance takes two weeks to decay, so to keep the temperature conditions in the adit stable, strict restrictive measures must be observed.

Our objective was to study ground motions at different frequencies to determine the parameters of the free and tidal oscillations of the Earth and assess the

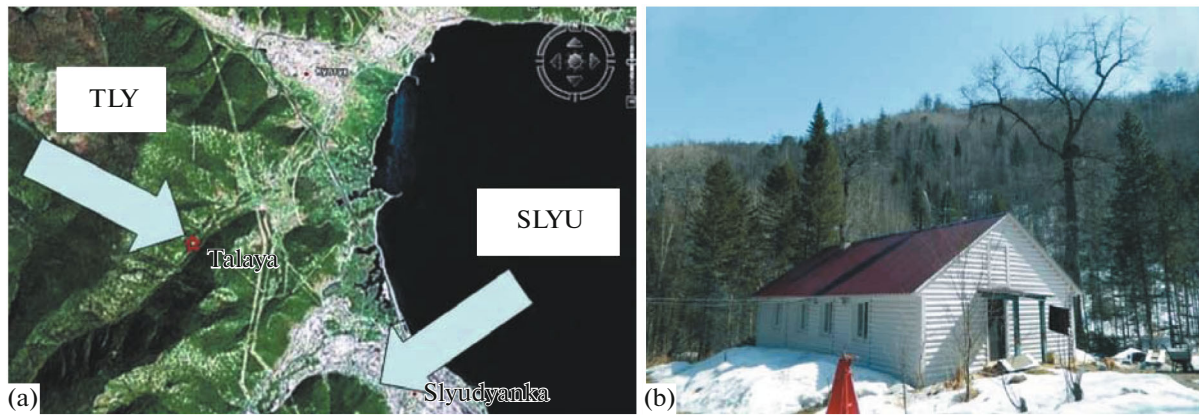


Fig. 1. Location of Talaya seismic station (TLY) and the town of Slyudyanka (SLYU) on the lakeside of Baikal (a) and the building of the station (b).

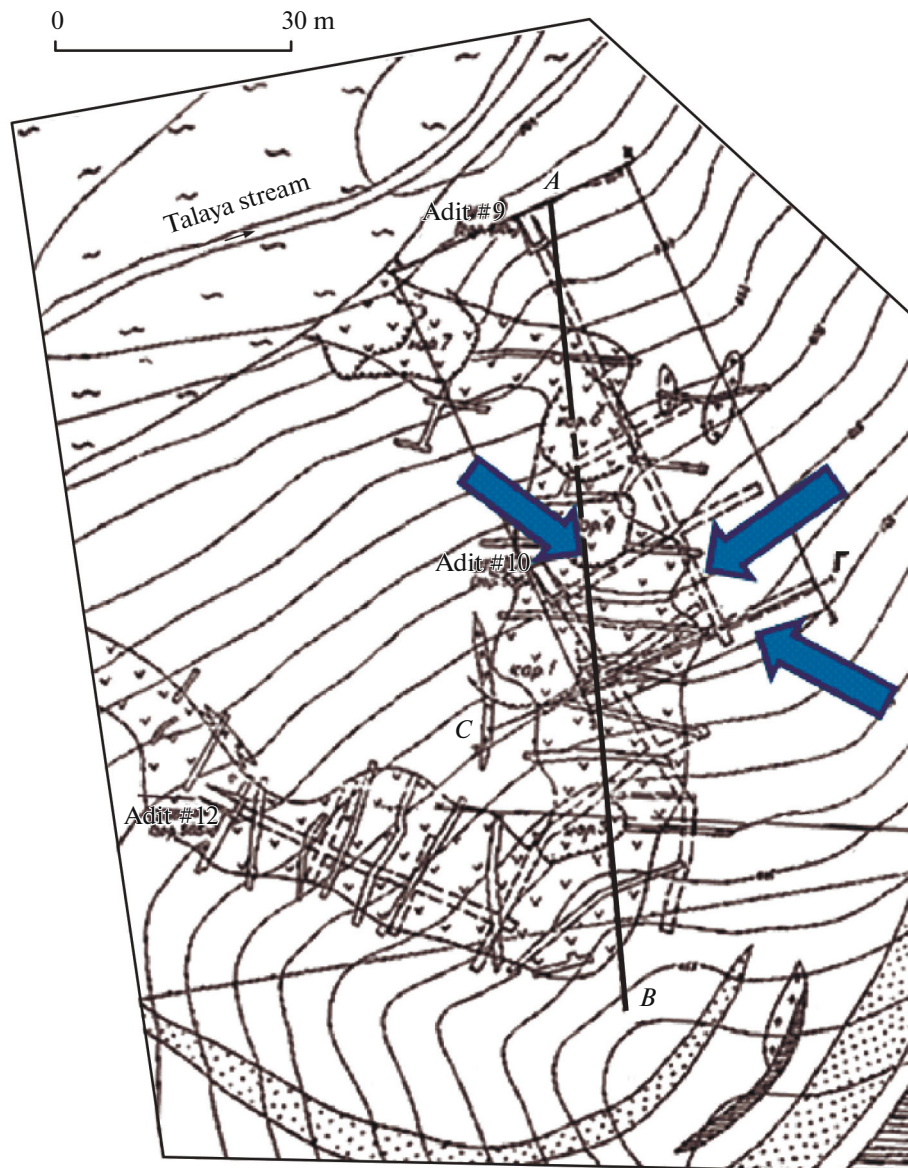


Fig. 2. The layout of Adit (No. 9) used for geophysical measurements at the Talaya seismic station. The arrows indicate drifts where strainmeters are installed. Rocks are represented by sedimentary deposits (moraine) along the Talaya valley and underlying Archean marbles with inclusions of granite-gneiss intrusions.

effects of regional earthquakes in the Baikal rift system.

MEASUREMENT TECHNIQUES AND INSTRUMENTATION

High-precision strain measurement is a challenging problem as far as an earthquake-prone region is concerned. There are certain requirements in that case:

- (1) High sensitivity and high stability of instruments,
- (2) Low level of noise,
- (3) Representativeness of measurement data,
- (4) Instruments should be made as simple as possible, their installation and maintenance costs should be reasonable (Mogi, 1985).

Let us analyze the strain measurements made at the Talaya seismic station from 1989 to 2015.

Quartz and invar rod strainmeters (from 1.3 m to 8.3 m long) were installed horizontally and vertically (Fig. 3) in a 20 m long lateral gallery at a distance of 90 m from the adit portal (Timofeev et al., 1994). Welded quartz pipes 1.3 to 2.0 m long, 32 mm in diameter, and 4 mm in wall thickness, were rigidly anchored at one end, the other end with an inductive sensor was placed on a pedestal unfixd. An 8.3 m-long invar rod strainmeter (25 mm in diameter) consists of rigidly connected 1.5-m sections with joints supported by quartz rollers placed on additional pedestals (see Fig. 3). A system was used with a sine wave generator (a two-cycle relaxation oscillator, frequency 20 kHz) and an inductive sensor as load for recording displacements. The inductive sensor is composed of two coils mounted on a micrometer table, with a movable core fixed on the strainmeter rod. Provided that the displacement $\Delta x \ll l_0$, the sensitivity S can be written as follows (Asch et al., 1991):

$$S = \Delta L / \Delta x = (4\mu_0 N^2 s / l_0^2) \Delta x \left[1 + (2\Delta x / l_0)^2 + \dots \right]. \quad (1)$$

The sensitivity of the sensor depends on the initial position l_0 of the coating (distance between the coils of the sensor): the smaller l_0 , the greater the sensitivity. If the displacement Δx is much smaller than l_0 , only then the sensitivity can be considered to be a constant parameter. Therefore, these sensors can only be used to record displacements of about a millimeter. This system retains its linearity within a narrow range of displacements. Typically, the gap between the coils is from 1 to 2 mm. A strainmeter with a baseline of 1 to 10 m detects displacements between 5×10^{-5} and 5×10^{-4} mm if tidal deformations are of up to 5×10^{-8} . The condition that the displacement should be much smaller than the gap between coils is perfectly satisfied. Moreover, this condition also works if the annual strain rate is no higher than 10^{-6} ; displacements vary from 10^{-3} to 10^{-2} mm at that. The measurement range

of the rod strainmeter was determined using a micrometer mounted on a unique two-coordinate micrometer table, displacements being from 0.01 and 0.02 mm. According to Talaya adit-based measurement data, the range error was usually about 5%. Strain measurements, at the seismic station located at a distance of 30 meters from the adit, were recorded by an analog recording system (see Fig. 1b). Such systems were used between 1989 and 1995.

The adit of the Talaya seismic station used both rod and laser strain measuring systems. Laser digital systems have operated in a continuous recording mode since 1995. Let us briefly describe the laser strainmeter installed in the adit of the Talaya seismic station (Bagaev et al., 1992). This instrument is a heterodyne phase-sensitive laser displacement meter for measuring small displacements using long baselines. It has a similar design to a two-frequency interferometric system with two phase-locked lasers (Bagaev et al., 1992). The system was developed at the Institute of Laser Physics, Siberian Branch, Russian Academy of Sciences (ILP SB RAS). It continuously records wave phase changes caused by the Doppler effect when a laser beam is reflected off a moving object so that the displacement is as follows:

$$\Delta l = (\Delta\varphi(t) / 2\pi) \lambda / 2 = (\lambda / 4\pi) \int_0^T \Omega(t) dt, \quad (2)$$

where Δl is the recorded displacement, $\Delta\varphi(t)$ is the phase difference, $\Omega(t)$ is the Doppler frequency shift that depends on time, and T is the measurement time. The laser displacement sensor also has a forming and receiving optical unit and a recording computer complex.

The sensitivity of the open-type laser system is limited by atmospheric pressure variations, under the conditions in the adit at a stable temperature (daily variations of 0.001°C). The capabilities of the system, to estimate the differential deformation, were first demonstrated using two orthogonal arms (baseline 25 m). Later, a laser interferometric system with a supporting compensation arm was developed and experimentally tested (Fig. 4). It was possible to exclude the influence of slow diurnal meteorological variations without special shielding of the two measuring arms and increase the relative sensitivity to displacements in a wide frequency range by more than three orders of magnitude, reaching value from 10^{-9} to 10^{-11} . The laser strain metering system makes it possible to record earthquakes, the free and tidal oscillations of the Earth, seiches in Lake Baikal, deterministic diurnal variations of microdeformation noise, and crustal deformation processes related to seismic activity (Fig. 5).

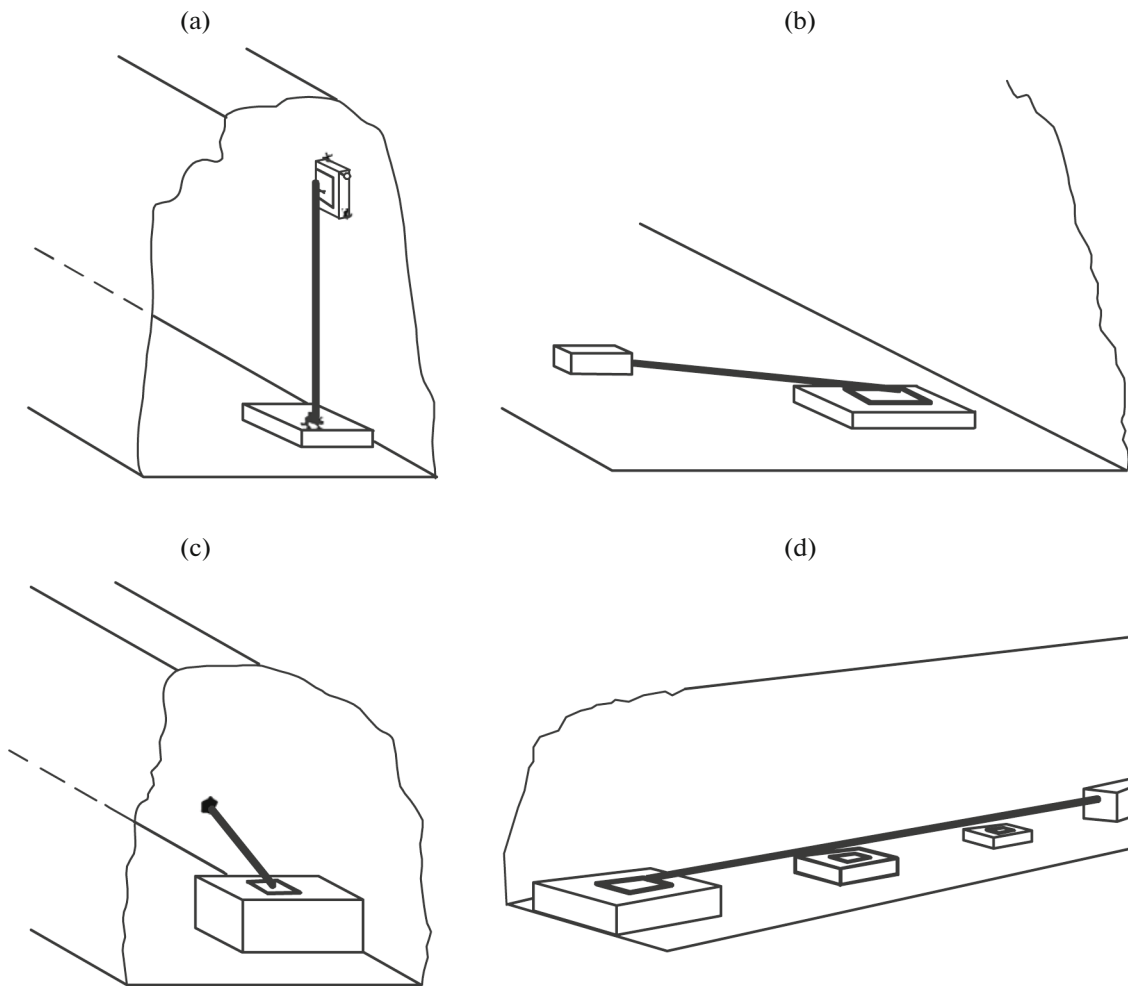


Fig. 3. Rod strainmeters in the adit of the Talaya station. The free end is on a two-coordinate micrometer table where the inductive sensor is placed: (a) vertical quartz strainmeter (1.6 m); (b) horizontal quartz N-S strainmeter (1.3 m); (c) horizontal quartz E-W strainmeter (2.0 m); (d) horizontal 8.3m-long invar-rod strainmeter (azimuth -22.5° N) with rollers, additional pedestals placed under the joints.

MEASUREMENT RESULTS AND EVALUATION OF ELASTIC MODULI OF ROCKS

Based on measurements of short-period variations caused by atmospheric pressure jumps, the effective elastic modulus of rocks (marble) was estimated. A quartz pressure transducer (Gridnev, 1975) and rod strainmeter allow the in-situ determination of rock mass characteristics. During the fast propagation of atmospheric front variations at periods of a few minutes to an hour were recorded (Gridnev and Timofeev, 1990, 1991). So the effective elastic modulus was evaluated as follows: $\mu = 4.73 \times 10^9 \pm 0.21 \times 10^9$ Pa. Based on the petrophysical analysis and ultrasonic measurements on core samples taken from a well located at a distance of 150 m from the adit portal, P and S wave velocities were estimated: $V_p = 4.16 \times 10^3$ m/s; $V_s = 2.62 \times 10^3$ m/s. The velocities and marble density $\rho = 2.87 \times 10^3$ kg/m³ give the shear elastic modulus $\mu =$

19.7×10^9 Pa. The difference in the values of elastic moduli indicates the cavity effect (Fig. 6) (Harrison, 1976; Blair, 1977; and Takemoto et al., 2006). Thus, for example, an adit with a cross-sectional height-to-width ratio of about 1 will exhibit a strain anomaly $e_{zz}^c \cong 3e_{zz}$. In our case, this is almost fourfold, which can be due to an additional contribution of rock mass fracturing.

The adit is on the northern side of a mountain valley and cannot be affected by spring flood because the depth of frost penetration is up to 1.5 m there. Soils thaw out in July and August; during heavy rains, there is water dripping in the adit, which increases humidity.

COSEISMIC DEFORMATIONS

The most rapid and significant changes in the deformation behavior were recorded after Novem-

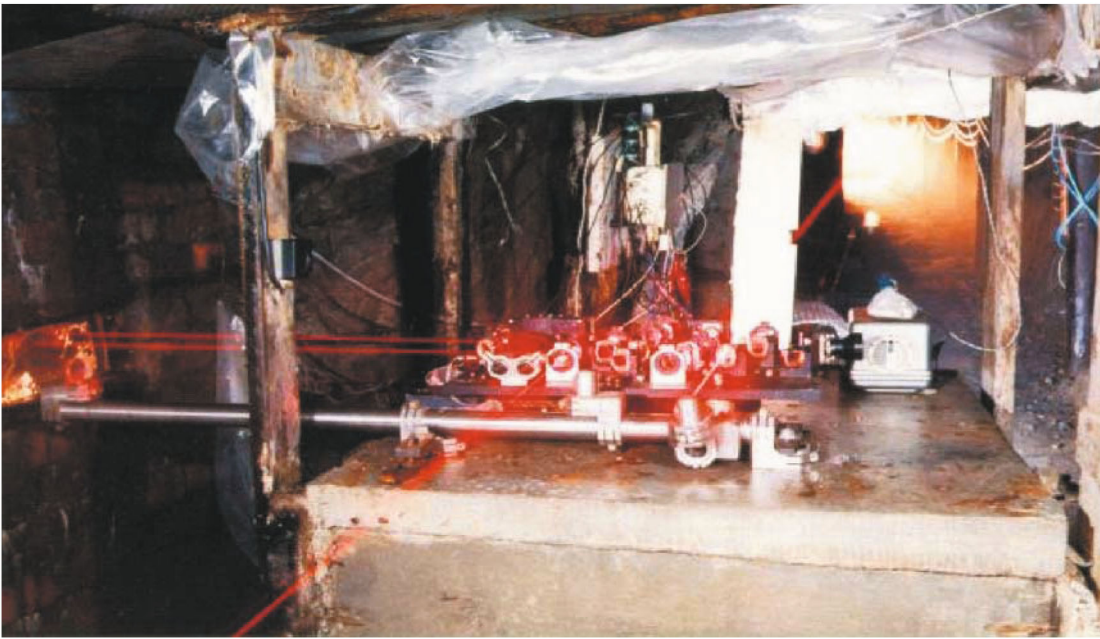


Fig. 4. Two-channel laser strainmeter with baselines of 25 m and a compensation shoulder (1 m), Talaya seismic station adit.

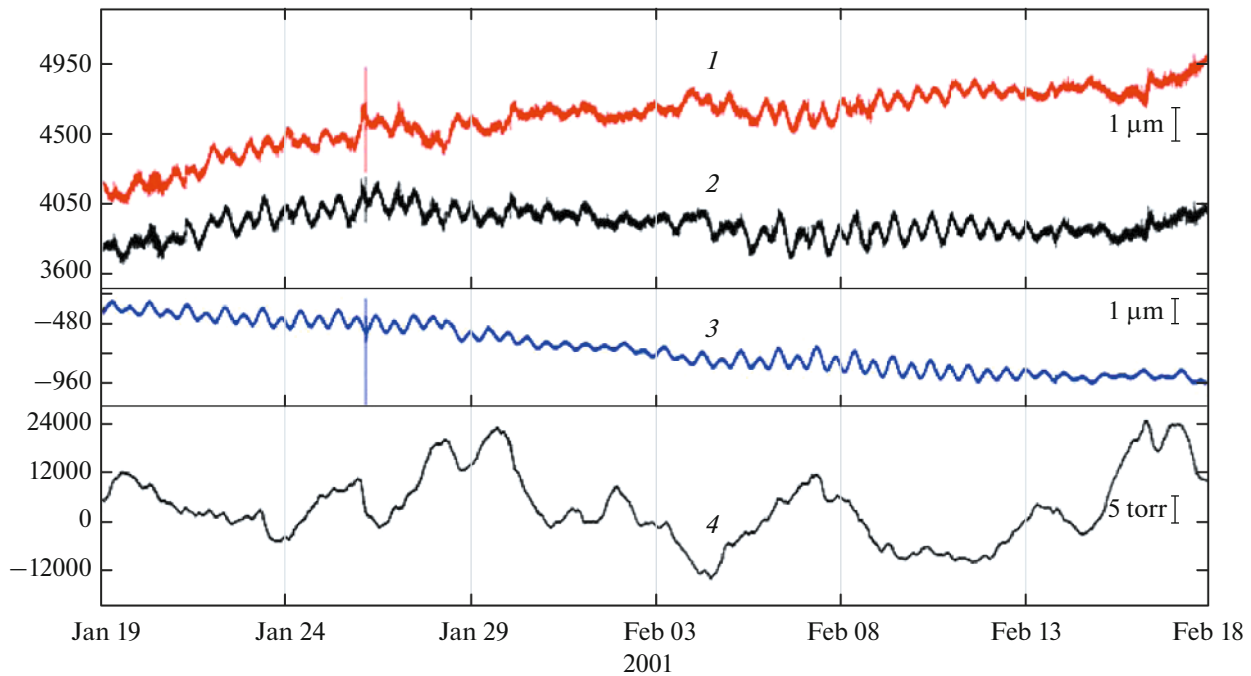


Fig. 5. Laser strainmeter records 1 month long: (1) in azimuth of -24° N, (2) in azimuth of 66° N, (3) differential deformation, and (4) atmospheric pressure variation.

ber 27, 2008, Kultuk earthquake, with a magnitude of 6.3 on Richter scale, its epicenter is at a distance of 25 km from the Talaya seismic station. Figure 7 shows the deformation behavior before the event. The earthquake caused the brick chimneys and stoves in the

one-story wooden building of the seismic station to collapse. The earthquake caused power outage, hence the coseismic jump in volumetric deformation was evaluated using strainmeter data, tilt, and water-level measurement data. The coseismic strain was equal to

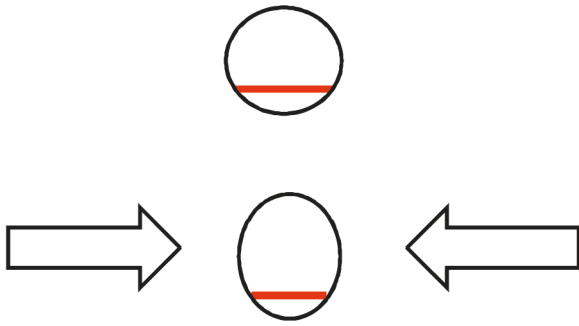


Fig. 6. Cavity effects in the adit due to the use of an instrument with a small baseline

for volumetric strain changes. Rod strainmeter data are graphically represented, for the period 1989–1995 and laser strainmeter data for the period 1995–2015.

The average strain rate (averaged over 25 years of measurement) is approximately the same as the strain rate derived from space geodesy data (Sankov et al., 1999; Likhnev et al., 2010) at baseline lengths of 10–50 km (Fig. 9). Note that the Kultuk earthquake (coordinates 51.62° N, 104.06° E, $M = 6.3$, depth 13 km, 25 km from the Talaya station) had the greatest influence on the deformation behavior, as opposed to more distant earthquakes that produced much smaller effects (Table 1).

1×10^{-6} . It allows the epicenter to be located more accurately and an earthquake model to be developed, with data on coseismic 3D displacements (Fig. 8).

Strain measurements along two orthogonal lines on the Earth’s surface allow the estimation of surface, volumetric, and vertical strains. For an isotropic medium we have:

$$\epsilon_{\text{volumetric}} = (\epsilon_{xx} + \epsilon_{yy})(1 - 2\nu)/(1 - \nu), \quad (3)$$

where $\epsilon_{\text{volumetric}}$ is the volumetric strain; ϵ_{xx} and ϵ_{yy} are the horizontal strains along two orthogonal axes, and ν is Poisson’s ratio.

Two orthogonal axes (north-west and east-west; –24° N and 66° N) were monitored from 1989 to 2015

TIDAL ANALYSIS

Let us analyze tidal variations. The response of the Earth to tidal forces produces important information about the internal structure of the Earth (Melchior, 1966). One of the methods for tidal studies involves using ground-based stations to monitor linear tidal deformations. Analysis of the results produces Love and Shida numbers (h and l) related to deformations and elastic parameters of the medium. Theoretical load Love and Shida numbers are derived from the Earth’s tidal deformation, calculated through the instrumentality of complex differential equations and are connected with the distribution of density and rigidity modulus (Table 2). Theoretical models of Earth’s deformation are based on the magnitude of the

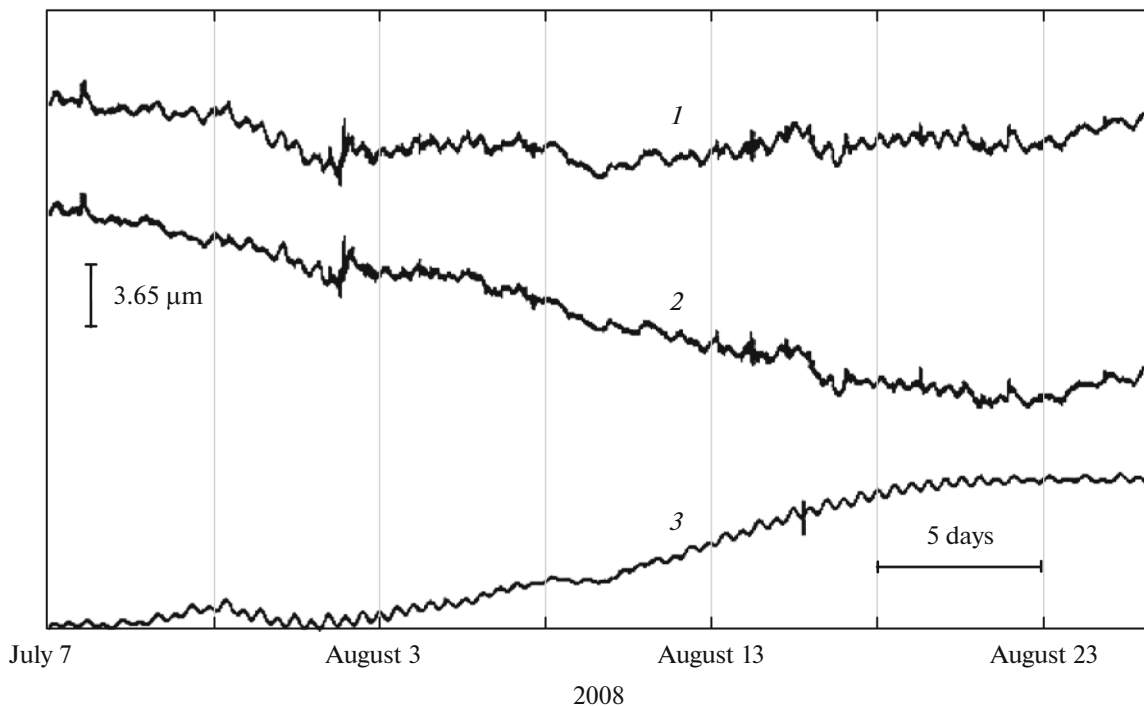


Fig. 7. Strainmeter (25 m) measurements made in Talaya seismic station adit a month before the Kultuk earthquake (August 27, 2008): deformation behavior (1) in azimuth of –24° N and (2) in azimuth of 66° N, and (3) differential deformation.

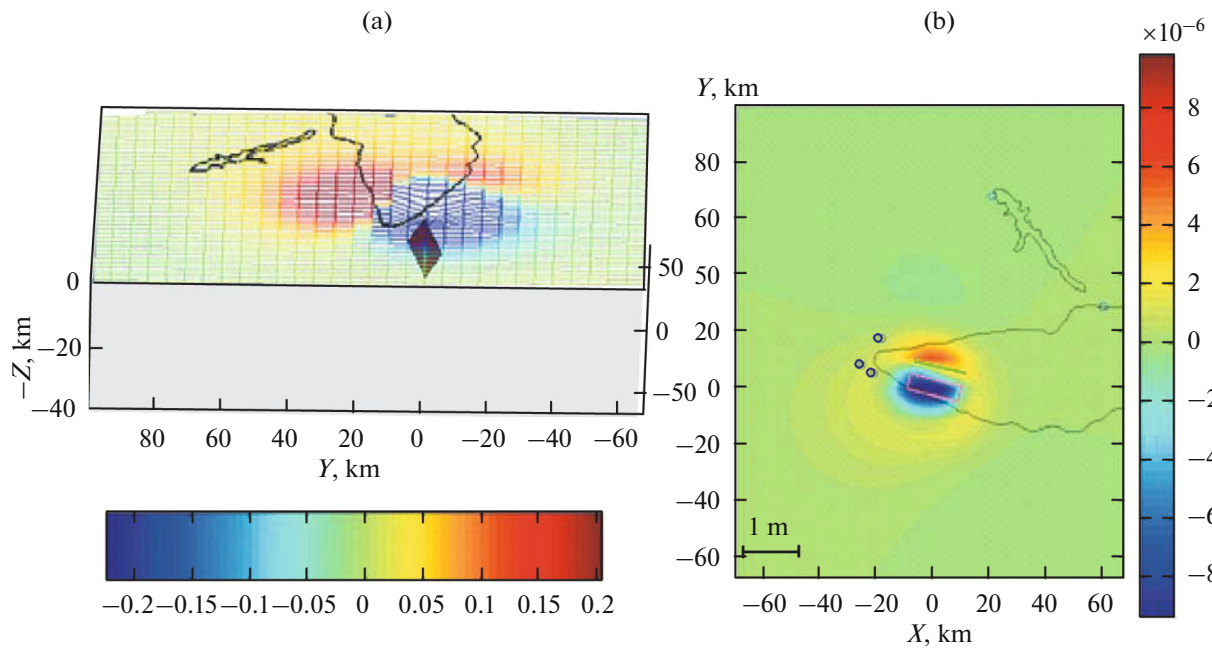


Fig. 8. Model of coseismic displacements and deformations during the Kultuk earthquake: (a) vertical displacements and (b) distribution of coseismic volumetric strain. According to experimental data, coseismic jump at the Talaya station is $\Delta N = -2 \pm 2 \text{ mm}$, $\Delta E = +10 \pm 2 \text{ mm}$, $\Delta H = -15 \pm 2 \text{ mm}$, and $\Delta \epsilon = +1 \times 10^{-6}$. Special software (Toda et al., 2011) was used in computations.

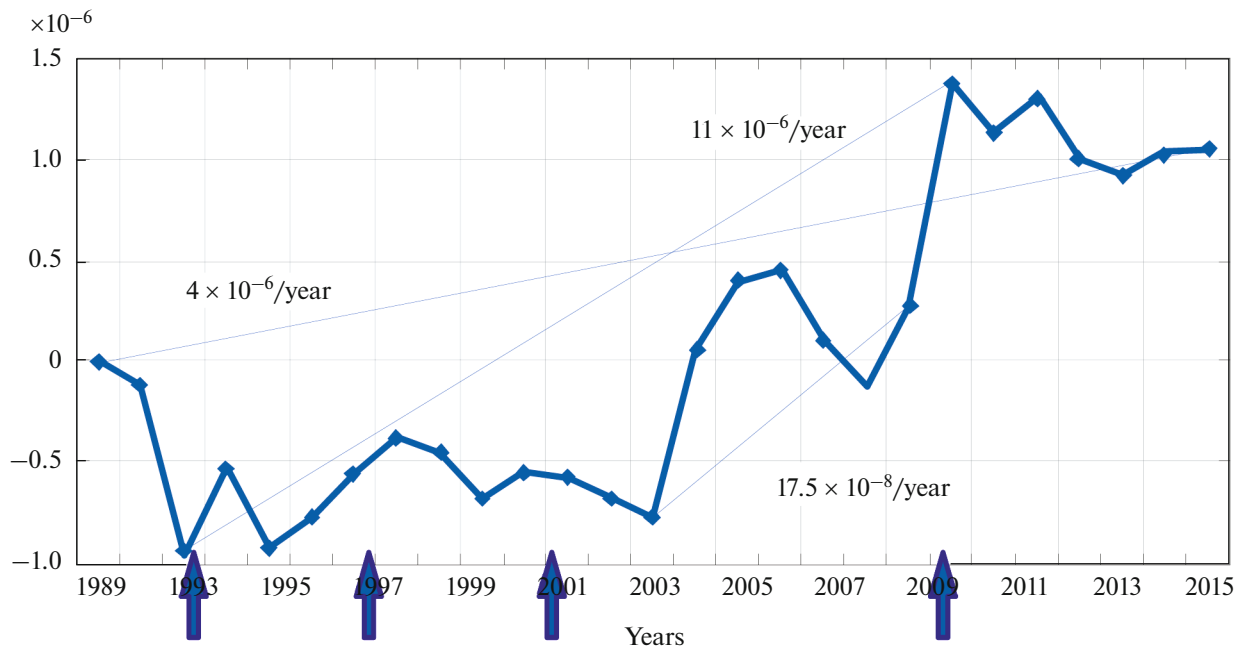


Fig. 9. Volumetric strain variations based on strainmeter measurements in Talaya adit. The arrows indicate strong regional earthquakes ($M > 5$) that occurred in the vicinity of the Talaya seismic station (Table 1). The December 27, 1999, Busingol earthquake ($M = 6.7-7.0$) occurred 200 km to the west of the Talaya station.

tidal force, which is evaluated with an accuracy of 10^{-7} based on astronomical observations, and different models of the Earth's structure (Melchior, 1966; Molodenskii, 1984, 2001). The tidal analysis was exe-

cuted using internationally recognized programs (Wenzel, 1996). Input data were thoroughly selected.

Tables 3 to 7 show the results of the tidal analysis for different strain components. Note that the semi-di-

Table 1. Strong earthquakes ($M > 5.5$) recorded in the vicinity of the Talaya station (1994–2015)

Earthquake time and coordinates	Magnitude	Distance to the epicenter (km) and range of magnitudes	
		$0 < L < 50$	$50 < L < 100$
June 29, 1995; 51.71° N, 102.70° E	5.5–5.7		67 km to the west
February 25, 1999; 51.63° N, 104.89° E; 51.65° N, 104.80° E; 51.58° N, 104.78° E	5.5–5.8		86 km to the east
August 27, 2008; 51.61° N, 104.07° E	6.3–6.5	25 km to the east	

urnal lunar wave M2 (E-W) has a small theoretical amplitude in nanostrains (10^{-9}) at the latitude of the Talaya stations: $O1 = 6.82$, $K1 = 9.59$, $M2 = 0.37$, and $S2 = 0.17$; the result reflects noise analysis.

The analysis shows that the amplitude factor is about 1, i.e., it is equal to the theoretical value. Deviations can be explained by the inaccurate installation of the instrument, the complexity of instrument calibration during many years, and power supply instability. In the case of analog recording systems, diurnal temperature variations could affect a 30-meter signal cable from the adit portal to the station building. Laser-based systems can be affected by seasonal humidity variations in the adit. Therefore, the results concerning diurnal waves O1 and K1 may be inaccurate, especially for phase shifts. Note a positive value ($+9^\circ$) of the phase shift for the most reliably detected semidiurnal wave M2 (see Tables 3 and 6). The same effect observed in tilt measurement data (Timofeev et al., 2020) is evidence of the influence of the Main Sayan fault, which separates the Siberian platform and the Baikal rift zone, on the tidal deformations observed at the Talaya station.

Table 2. Models of the Earth’s structure and load Love and Shida numbers derived from calculated tidal deformation of the Earth (Melchior, 1966; Molodenskii, 1984; and Dehant et al., 1999)

Model of the Earth	Love number h	Shida number l
Gutenberg	0.6055	0.0829
Hilbert–Dziewonsky (PREM)	0.6130	0.0853
Dehant–Defraigne–Wahr DDW99	0.6206	0.0904

With respect to directions beyond the main axes (north-south and east-west), the tidal analysis produces the ratio of Love and Shida numbers (l/h) independent of the calibration error (Tables 8 and 9).

The tables show the results of the analysis of the measurements made with our strainmeters and an OZAWA strainmeter installed in a kilometers-long adit at Walferdange (a suburb of Luxembourg), at the International Center for Geodynamics and Seismology.

Altogether, within the limits of observation error, the observed values are in good agreement with the theoretical mechanical parameters of the modern Wahr–Dehant model (Dehant et al., 1999) and the PREM model of the Earth (Dziewonski and Anderson, 1981), the inelasticity of the Earth’s mantle taken into account (Table 10).

Long-term data analysis showed that differential deformation data are the most reliable for the estimation of Shida number. A complete set of Love and Shida numbers for intracontinental regions of Eurasia in middle latitudes is derived from gravimetric data (Timofeev et al., 2008; Ducarme et al., 2008) and experimental data: $h = 0.6077 \pm 0.0008$, $k = 0.3014 \pm 0.000$, and $l = 0.0839 \pm 0.0001$. Slight differences from the theoretical values are due to the disregard for the effects of the oceans. The empirical tidal parameters make it possible to calculate tidal deformations for the Baikal region using any components of deformation, tilt, and gravity. The quality of differential deformation data allows analyzing changes in tidal parameters (amplitude and phase) over time. We used average annuals for the period from 1995 to 2015 to exclude the influence of seasonal factors. Presented below are the analysis results (Figs. 10 and 11), showing periods of strong earthquakes; irreversible phase changes after the Kultuk earthquake reached 2 degrees, which can be attributed to changes in the properties of the Earth’s crust in the region (Beaumont and Berger, 1974).

Table 3. Tidal analysis data and their comparison with the theoretical amplitude, amplitude factor, and phase shift for the north-south component of quartz rod strainmeter (baseline length 1.3 m), 33456 hours of observations from July 1988 to December 1995

Wave	Observed amplitude	Model	Experiment	Difference	Error	Observed phase shift, deg	Phase error, deg
O1	4.56	1.000	1.071	+0.071	0.045	+1.81	2.41
K1	3.37	1.000	1.059	+0.059	0.031	-3.49	1.71
M2	10.81	1.000	1.007	+0.007	0.006	+9.37	0.48
S2	5.39	1.000	1.080	+0.080	0.012	+4.97	0.92

Table 4. Tidal analysis data and their comparison with the theoretical amplitude, amplitude factor, and phase shift for the east-west component of quartz rod strainmeter (baseline length 1.3 m), 720 hours of observations from July 1988 to June 1991

Wave	Observed amplitude	Model	Experiment	Difference	Error	Observed phase shift, deg	Phase error, deg
O1	6.42	1.000	0.947	-0.0529	0.045	-24.44	2.76
M2	6.43	1.000	16.348	+15.3481	0.626	-3.98	2.19

EARTH'S FREE OSCILLATIONS

The study of the Earth's free oscillations is one of the important areas of geophysics. The Earth's free oscillations, during catastrophic earthquakes with a magnitude greater than 8, can be detected with laser strainmeters. (Fig. 12). From an experimental point of view, the free oscillations unite seismology and gravimetry. Strainmeter records (Jahr et al., 2006) after the Sumatran earthquake (December 26, 2004, $M = 9$) show the Earth's free oscillations at periods of 57 min, 35.5 min, 25.8 min, 20 min, 13.5 min, 11.8 min, 8.4 min and shorter. Let us consider the measurements made at the Talaya station during the catastrophic March 11, 2011 earthquake ($M = 9$) in Japan.

Figure 13 shows the deformation spectra. The spectra detected the frequencies of torsional and spheroidal oscillations (Zharkov, 1983). The Earth's core is

liquid; torsional oscillations are transverse oscillations (similar to transverse waves), so they affect only solid regions of the Earth and are determined by the distribution of density and rigidity modulus in the mantle and crust.

The Earth's free oscillations certainly "prefer" (a) the Gutenberg model with a layer of low seismic wave velocities at depths of 50–250 km, rather than (b) the Jeffries model with no such layer. Different frequency intervals are accounted for by different regions of the Earth's interior. Therefore, we can use the free oscillations to study not only the integral properties of the globe, such as solid Earth tides but also differential properties. A laser strainmeter is highly instrumental in studying the Earth's free oscillations. Also, records of the strainmeter feature free oscillations of the surface of Lake Baikal, so-called seiches that periodically

Table 5. Tidal analysis data and their comparison with theoretical amplitude, amplitude factor, and phase shift for -22.5° N component of quartz rod strainmeter (baseline length 1.3 m), 20784 hours of observations from February 1990 to February 1995

Wave	Observed amplitude	Model	Experiment	Difference	Error	Observed phase shift, deg	Phase error, deg
O1	5.06	1.000	1.104	+0.104	0.070	+6.46	2.93
K1	6.53	1.000	1.014	+0.014	0.051	-1.59	2.84
M2	9.86	1.000	1.000	+0.000	0.034	-0.02	1.55
S2	5.14	1.000	1.120	+0.120	0.072	-7.76	2.99

Table 6. Tidal analysis data and their comparison with the theoretical amplitude, amplitude factor, and phase shift for laser strainmeter’s component with an azimuth of -24° N, 8496 hours of observations from January 1995 to December 1996

Wave	Observed amplitude	Model	Experiment	Difference	Error	Observed phase shift, deg	Phase error, deg
O1	4.89	1.000	1.010	+0.010	0.058	-10.1	3.3
M2	10.290	1.000	1.073	+0.073	0.022	+9.0	1.2

Table 7. Tidal analysis data and their comparison with theoretical amplitude, amplitude factor, and phase shift: laser strainmeter component with an azimuth of 66° N, 8496 hours of observations from January 1995 to December 1996

Wave	Observed amplitude	Model	Experiment	Difference	Error	Observed phase shift, deg	Phase error, deg
M2	4.60	1.000	1.099	+0.099	0.035	-0.08	2.05
S2	2.04	1.000	1.028	+0.028	0.080	+31.11	4.60

load the bottom of Lake Baikal, causing deformations of the Earth’s crust (*Atlas Baikala*, 1993). Among other causes, standing waves (seiches) in Lake Baikal result from strong earthquakes, abrupt changes in atmospheric pressure, and two weeks long tidal modulations.

Spectral analysis of the lake’s water level recorded at the Listvyanka (the source of the Angara River) shows the following periods: 4 h 33 min, 2 h 33 min, 1 h 28 min, and 1 h 06 min. From the southern part of the lake (the village of Kultuk), nodal lines of seiches are located at distances of 280, 130, 360, and 540 km,

respectively. Theoretically, the periods of seiches are as follows:

$$T_n = 2l / n\sqrt{gH}, \tag{4}$$

where l is the length of the lake; H is its average depth, normal gravity $g = 9.8 \text{ m/s}^2$, and n is the mode (1, 2, 3, etc.). The amplitude of the seiches has seasonal variations. Laser strainmeter records made at the Talaya station at a distance of 7 km from the lakeside revealed the periodic load of a water layer up to 15 cm thick on the lake bottom (Fig. 14).

Table 8. Observed and theoretical ratios of Love and Shida numbers l/h

Wave	Observed l/h	Theoretical l/h
Azimuth of -22.5°		
O1	0.1098 ± 0.0205	0.1466
M2	0.1455 ± 0.0110	0.1457
Azimuth of 66°		
O1	0.1550 ± 0.0745	0.1466
M2	0.1217 ± 0.0047	0.1457

Table 9. The ratio of Love and Shida numbers, l/h , based on the results of the tidal analysis of measurements made in Walferdange adit (Luxembourg) with OZAWA12 horizontal strainmeter with a baseline of 50 m, azimuth -37.80° , 115824-hour series

Wave	Observed l/h	Model
Diurnal		
O1	0.1615 ± 0.0007	0.1466
K1	0.1803 ± 0.0005	0.1756
Semidiurnal		
M2	0.1488 ± 0.0004	0.1457
S2	0.1580 ± 0.0008	0.1457

Table 10. Model-based and observed parameters of strong tidal waves, measurements made with different instruments differently oriented in the Talaya adit Corrections (+ 9°) are applied to laser observation data presented in the two last lines of the table

Instrument	Baseline length, m	Azimuth	Wave	Model	Experiment	Error
Quartz strainmeter	1.3	N-S	M2	1.0000	1.007	0.006
Quartz strainmeter	2.0	E-W	O1	1.0000	0.947	0.045
Invar strainmeter	8.3	-22.5°	M2	1.0000	1.000	0.034
Laser strainmeter	25.0	-24.0°	M2	1.0000	1.073	0.022
Laser strainmeter	25.0	+66°	M2	1.0000	1.099	0.035
Laser strainmeter	25.0	-33.0°	M2	1.0000	0.9292	0.007
Laser strainmeter	25.0	+57°	M2	1.0000	0.9195	0.011

In addition to the oscillations observed at Listvyanka (periods of 4.55, 2.55, 1.47, and 1.1 h), spectral analysis of winter and summer observations reveals oscillations with a period of 3.4 h (205.5 min). The summer frequency spectrum is more elaborate, which is probably due to the filtration properties of the ice layer on Lake Baikal in winter. In the future, to develop a dynamic model of the water level of Lake Baikal, oscillations at the periods of seiches can be used. These periods should be taken into consideration during further analysis and interpretation.

CONCLUSIONS

Adit-based rod and laser strain metering systems are capable of recording geophysical processes in dif-

ferent frequency ranges: from seconds to several years. Analysis of the Earth's free oscillations observed in the adit of the Talaya seismic station (Baikal) shows that they agree with the PREM model of the Earth. The results concerning the tidal frequencies are in agreement with the DDW99 tidal model of the Earth (the viscosity of the mantle taken into account). From integrated data for intracontinental regions of Eurasia, a complete set of Love and Shida numbers were determined, at mid-latitudes: $h = 0.6077 \pm 0.0008$, $k = 0.3014 \pm 0.0001$, $l = 0.0839 \pm 0.0001$. Theoretical fields of tidal deformations to be imaged for the Baikal region are allowed by the resulting tidal parameters using different strain and tilt components and tidal variations in gravity. Atmospheric pressure variations and changes in strain determined the static elastic

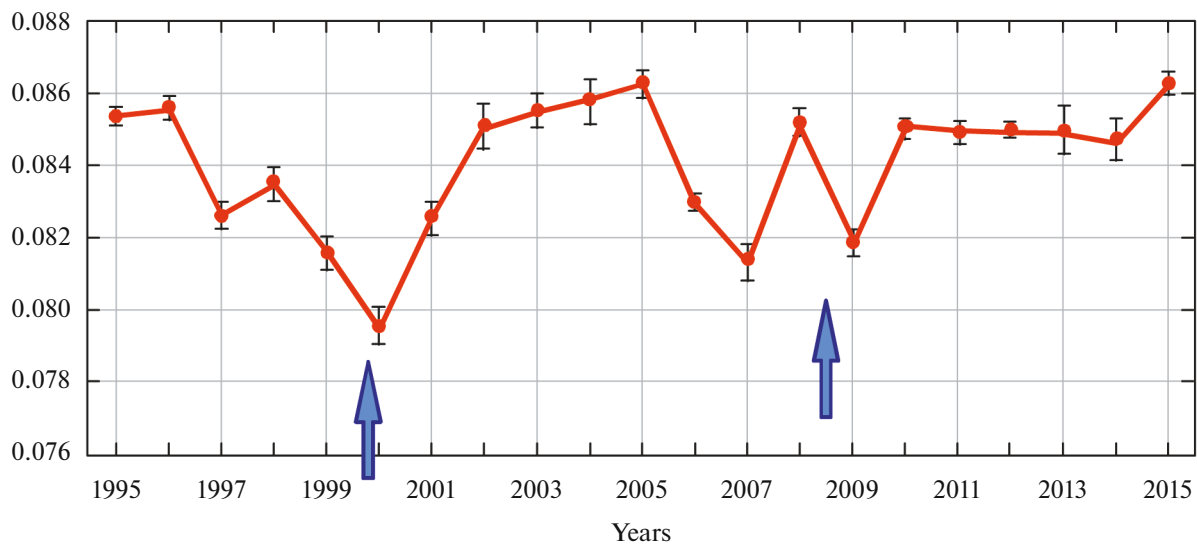


Fig. 10. Time-dependent variation of the Shida number derived from the amplitude factor of M2 wave based on annual laser strainmeter data. The error level is shown. Arrows indicate the period of 1999–2000 and 2008 earthquakes (see Table 1).

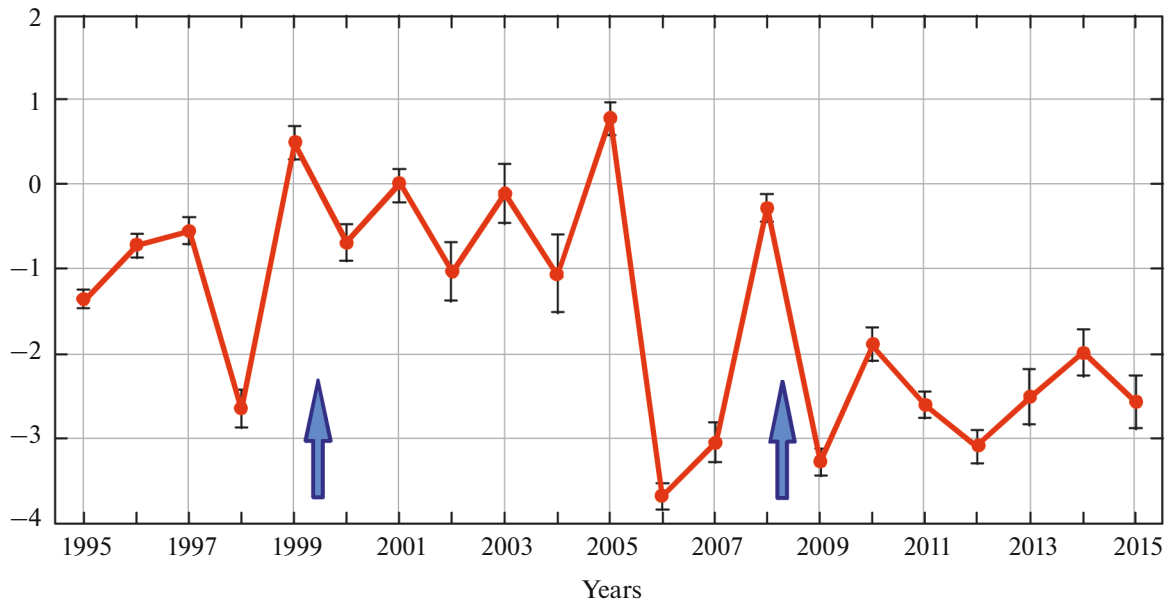


Fig. 11. Time-dependent phase-shift variation of M2 wave in degrees: The period after the earthquake of 2008 is discernible as well as transition to a new level, which indicates a change in physical properties of rocks during near earthquakes (see Table 1).

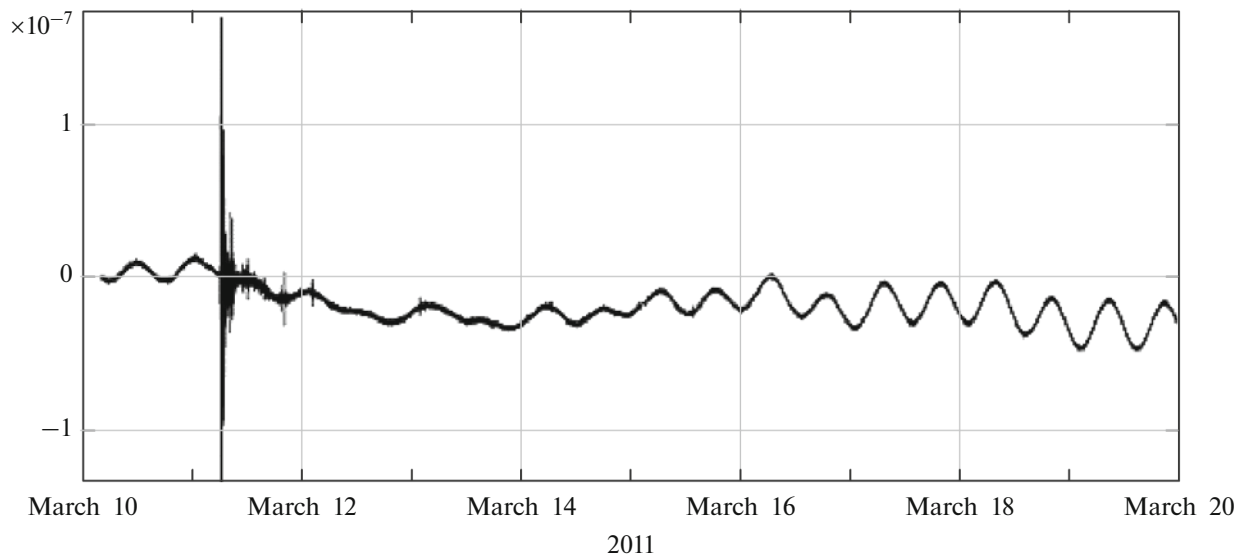


Fig. 12. Unfiltered differential signal record (strainmeters in azimuths of -24° N and 66° N, the Talaya seismic station, Lake Baikal): the effect of the March 11, 2011 earthquake, arrival of body waves, the Earth's free oscillations, and tidal variations. The y-axis represents strain, the x-axis is time (March 2011).

moduli of the rock mass. It is found that the static elastic moduli derived from the strainmeter measurement data are 4 times smaller than those obtained by ultrasonic examination of core samples, which is due to the cavity effects (adit configuration) and rock fracturing. The spectrum of laser strainmeter measurement data revealed free oscillations of the surface of Lake Baikal (seiches). Long-term volumetric strain variations feature periods of strong

earthquakes ($M > 5.5$). Coseismic changes in volumetric strain and the annual strain rate are estimated for the Kultuk earthquake that occurred at a distance of 25 km from the seismic station. Changes in the amplitude and phase of strain, based on the results of the tidal analysis, are plotted for twenty years. Periods of strong approaching earthquakes are seen in the plots; the Kultuk earthquake changed the phase shift by irreversible 2° .

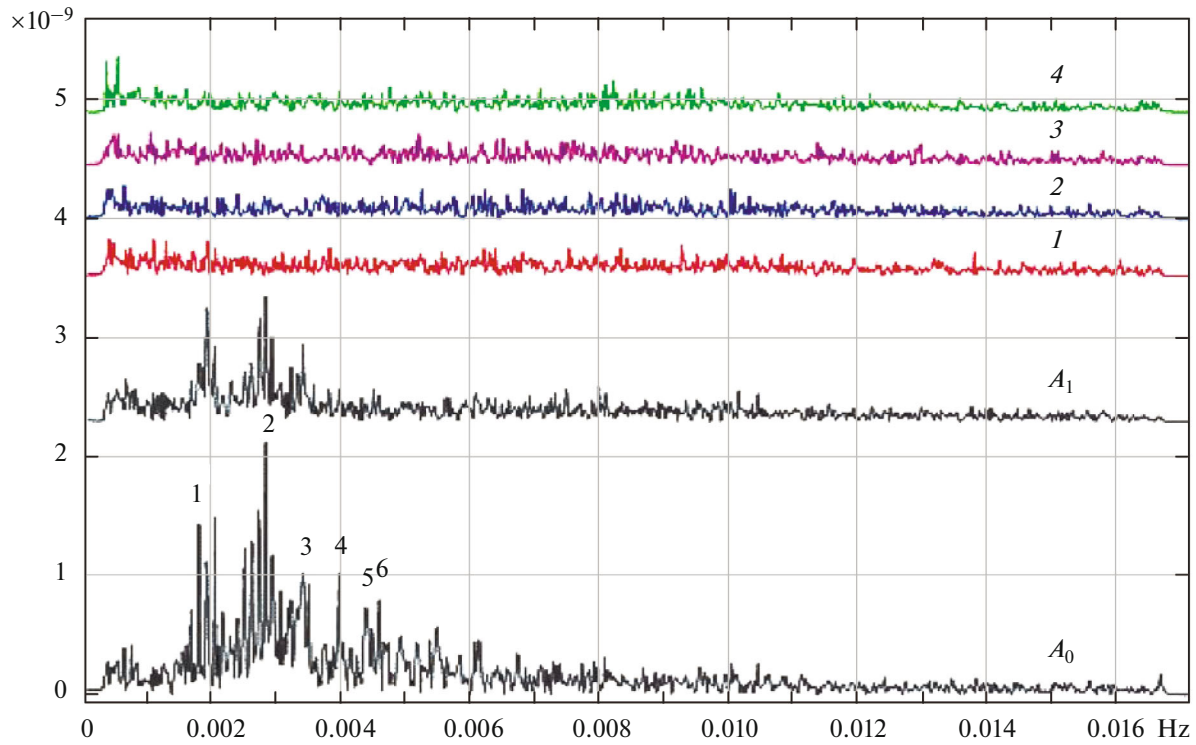


Fig. 13. Spectra of differential signals: (A_0) immediately after the earthquake of March 11, 2011; (A_1) shifted by 3 hours; (I) shifted by 24 hours; (2) shifted by 48 h, (3) shifted by 72 h; (4) shifted by 96 h. Clearly visible are peaks at the frequencies from 0.h to 0.0060 Hz (57 min—0.00029 Hz; 35.5 min—0.00047 Hz; 25.8 min—0.00065 Hz; 20 min—0.00083 Hz; 13.5 min—0.00123 Hz; 11.8 min—0.00141 Hz) and then peaks 9.0 min (I), 6.1 min (2), 4.9 min (3), 4.2 min (4), 3.8 min (5), and 3.6 min (6). The y-axis represents deformation; the x-axis is frequency, Hz.

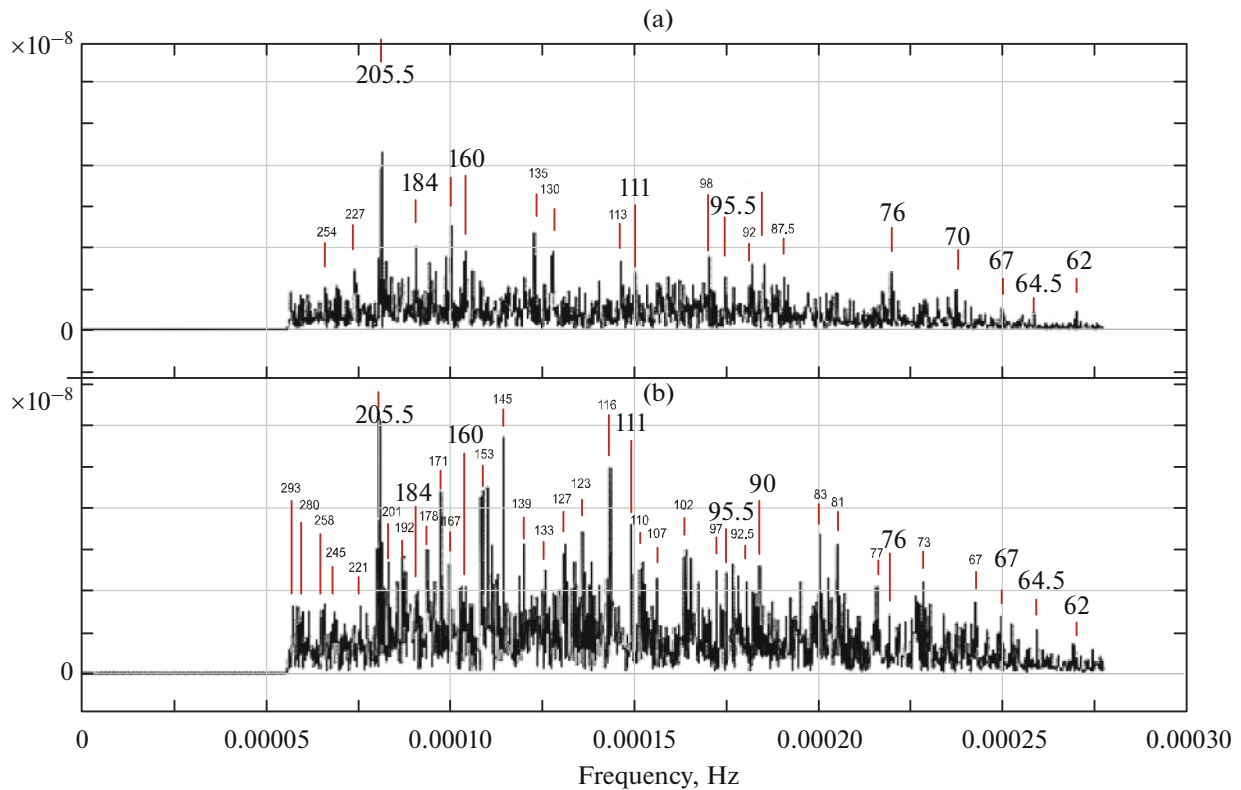


Fig. 14. Spectra of laser strainmeter measurement data obtained in the adit of the Talaya seismic station in summer and winter. The x-axis represents frequency, Hz. The periods of spectral lines are given in minutes.

REFERENCES

- Agnew, D.C., Strainmeters and tiltmeters, *Rev. Geophys.*, 1986, vol. 24, no. 3, pp. 579–624.
- Asch, G., et al., *Les capteurs en instrumentation industrielle*, Paris: BORDAS, 1991, vol. 1.
- Atlas Baikala* (Atlas of Baikal), Moscow: Ross. Akad. Nauk, 1993.
- Bagaev, S.N., Orlov, V.A., Fomin, Yu.N., and Chebotaev, V.P., Heterodyne laser strainmeters for precise geophysical measurements, *Fiz. Zemli*, 1992, no. 1, pp. 85–91.
- Beaumont, C. and Berger, J., Earthquake prediction: Modification of the earth tide tilts and strains by dilatancy, *Geophys. J. R. Astron. Soc.*, 1974, vol. 39, pp. 111–121.
- Benioff, H., A linear strain seismograph, *Bull. Seismol. Soc. Am.*, 1935, vol. 25, no. 4, pp. 283–309.
- Blair, D., Topographic, geologic and cavity effects on the harmonic content of tidal strain, *Geophys. J. R. Astron. Soc.*, 1977, vol. 48, pp. 393–405.
- Boyersky, E.A., Ducarme, B., Latynina, L.A., and Vandercoilden, L., An attempt to observe the Earth liquid core resonance with extensometers at Protvino observatory, *Bull. Inf. Mar. Terr.*, 2003, vol. 138, pp. 10987–11009.
- Chupin, V.A., Sea bottom tomography using shore-based laser strainmeters, in *Fizika geosfer. 11-i Vserossiiskii simpozium: Materialy dokladov* (Proceedings of the 11th All-Russia Symposium “Physics of the Geospheres”), Vladivostok, Russia, 2019, Vladivostok: Tikhookean. Okeanol. Inst. Dal’nevost. Otd. Ross. Akad. Nauk, 2019, pp. 205–208.
- Ducarme, B., Timofeev, V.Yu., Everaerts, M., Gornov, P.Y., Parovishnii, V.A., and van Ruymbeke, M.A., Trans-Siberian Tidal Gravity Profile (TSP) for the validation of the ocean tides loading corrections, *J. Geodyn.*, 2008, vol. 45, nos. 2–3, pp. 73–82.
- Dehant, V., Defraigne, P., and Wahr, J.M., Tides for a convective Earth, *J. Geophys. Res.: Solid Earth*, 1999, vol. 104, no. B1, pp. 1035–1058.
- Dziewonski, A.M. and Anderson, D.L., Preliminary reference Earth model, *Phys. Earth Planet. Inter.*, 1981, vol. 25, pp. 297–356.
- Gridnev, D.G., Quartz air density gauge, in *Prilivnye deformatsii Zemli* (Tidal Deformations of the Earth), Moscow: Nauka, 1975, pp. 130–140.
- Gridnev, D.G. and Timofeev, V.Yu., USSR Inventor’s Certificate no. 1557318, 1990, *Byull. Isobret.*, no. 14.
- Gridnev, D.G. and Timofeev, V.Yu., USSR Inventor’s Certificate no. 1668663, 1991, *Byull. Isobret.*, no. 29.
- Guseva, T.V., *Sovremennye dvizheniya zemnoi kory v zone perekhoda ot Pamira k Tyan’-Shanyu* (Contemporary Motions of the Earth’s Crust in the Transitional Zone between Pamirs and Tien Shan), Moscow: Inst. Fiz. Zemli Akad. Nauk SSSR, 1986.
- Harrison, J.C., Cavity and topographic effects in tilt and strain measurement, *J. Geophys. Res.*, 1976, vol. 81, pp. 319–328.
- Jahr, T., Kroner, C., and Lippmann, A., Strainmeters at Moxa observatory, Germany, *J. Geodyn.*, 2006, vol. 41, pp. 205–212.
- Latynina, L.A. and Karmaleeva, R.M., *Deformograficheskie izmereniya* (Measurements of Strains), Moscow: Nauka, 1978.
- Lukhnev, A.V., San’kov, V.A., Miroshnichenko, A.I., Ashurkov, S.V., and Calais, E., GPS rotation and strain rates in the Baikal–Mongolia region, *Russ. Geol. Geophys.*, 2010, vol. 51, no. 7, pp. 785–793.
- Melchior, P., *Earth Tides*, London: Pergamon, 1966.
- Mogi, K., *Earthquake Prediction*, Tokyo: Academic, 1985.
- Molodenskii, S.M., *Prilivy, nutatsiya i vnutrennee stroenie Zemli* (Tides, Nutation, and Internal Structure of the Earth), Moscow: Inst. Fiz. Zemli Akad. Nauk SSSR, 1984.
- Molodenskii, S.M., *Izbrannye trudy. Gravitatsionnoe pole. Figura i vnutrennee stroenie Zemli* (Selected Papers: Gravity Field, Shape, and Internal Structure of the Earth), Moscow: Nauka, 2001.
- Popov, V.V., Temperature deformations of the Earth’s surface, *Izv. Akad. Nauk SSSR. Fiz. Zemli*, 1961, no. 7, pp. 3–10.
- San’kov, V.A., Levi, K.G., Kale, E., Deversher, Zh., Lesne, O., Lukhnev, A.V., Miroshnichenko, A.I., Buddo, V.Yu., Zalutskii, V.T., and Bashkuev, Yu.B., Contemporary and Holocene horizontal motions in the Baikal geodynamic research area, *Geol. Geofiz.*, 1999, vol. 40, no. 3, pp. 422–430.
- Takemoto, S., Hideo, M., Akito, A., Wataru, M., Junpei, A., Masatake, O., Akiteru, T., Shinji, M., Takashi, U., Daisuke, T., Toshihiro, H., Souichi, T., and Yoichi, F., A 100 m laser strainmeter system in the Kamioka Mine, Japan, for precise observations of tidal strains, *J. Geodyn.*, 2006, vol. 41, pp. 23–29. <https://doi.org/10.1016/j.jog.2005.08.009>
- Timofeev, V.Yu., Sarycheva, Yu.K., Panin, S.F., Anisimova, L.V., Gridnev, D.G., and Masal’skii, O., Study of tilts and deformations of the Earth’s surface in the Baikal Rift Zone, *Geol. Geofiz.*, 1994, no. 3, pp. 119–129.
- Timofeev, V.Yu., Ducarme, B., van Ruymbeke, M., Gornov, P.Yu., Everaerts, M., Gribova, E.I., Parovishnii, V.A., Semibalamut, V.M., Woppelmann, G., and Ardyukov, D.G., Transcontinental tidal transect: European Atlantic coast–Southern Siberia–Russian Pacific coast, *Izv., Phys. Solid Earth*, 2008, vol. 44, no. 5, pp. 388–400.
- Timofeev, V.Yu., Timofeev, A.V., Ardyukov, D.G., and Boyko, E.V., Quartz tiltmeters and their use in geophysical studies, *Seism. Instrum.*, 2020, vol. 56, no. 2, pp. 134–151. <https://doi.org/10.21455/si2019.3-2>
- Toda, Sh., Stein, R., Lin, J., and Sevilgen, V., *Coulomb 3.3 Graphic-Rich Deformation and Stress-Change Software for Earthquake, Tectonic, and Volcano Research and Teaching—User Guide*, U.S. Geol. Surv. Open-File Rep. 2011–1060, 2011. <https://pubs.usgs.gov/of/2011/1060/>. Accessed May 31, 2020.
- Wenzel, H.-G., The nanogal software: Earth tide data processing package ETERNA 3.30, *Bull. Inf. Mar. Terr.*, 1996, vol. 124, pp. 9425–9439. <https://doi.org/10.1016/j.jog.2005.08.017>
- Zharkov, V.N., *Vnutrennee stroenie Zemli i planet* (Internal Structure of the Earth and Planets), Moscow: Nauka, 1983.

Translated by B. Shubik